Supplementary information

Mapping the Catalytic Landscape of Doped Pd (111) for Formic Acid Synthesis Via CO_2 Hydrogenation Using First-Principles, Microkinetics, and SISSO Descriptors

Zhihong Zhang,†[a] Qingbo Wang,†[b] FeiFeng Wu,[c] Jiaqiang Yang,[d] Yi Yu,[a] Aimin Zhang,*[c] Shan Bin*[a]

[a] School of Materials Science and Engineering, Huazhong University of Science and Technology, Wuhan 430074, PR China

[b] School of Mathematics and Physics, China University of Geosciences (Wuhan), Wuhan, 430074, China

[c] State Key Laboratory of Precious Metal Functional Materials, Kunming, Yunnan 650106, China

[d] Zhongyuan critical metals laboratory, Zhengzhou University, Zhengzhou 450001, Henan, China

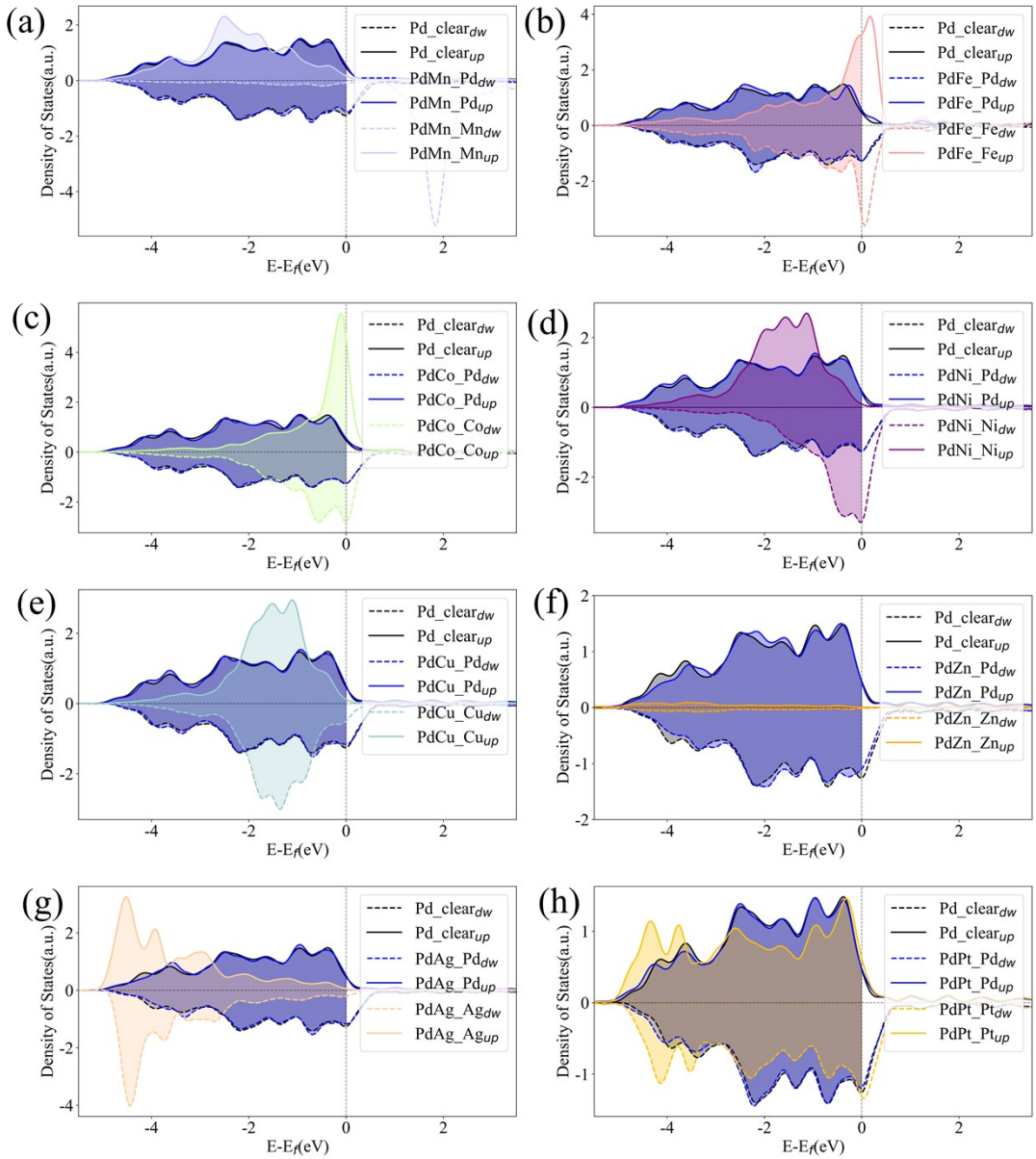

Figure S1. Projected Density of States (PDOS) of d-orbitals for Pd and dopant transition-metal (M) atoms on Pd(111)-M alloy surfaces (M = Mn, Fe, Co, Ni, Cu, Zn, Ag, Pt). (a)–(h) correspond to Pd(111)-Mn, Pd(111)-Fe, Pd(111)-Co, Pd(111)-Ni, Pd(111)-Cu, Pd(111)-Zn, Pd(111)-Ag, and Pd(111)-Pt surfaces, respectively.

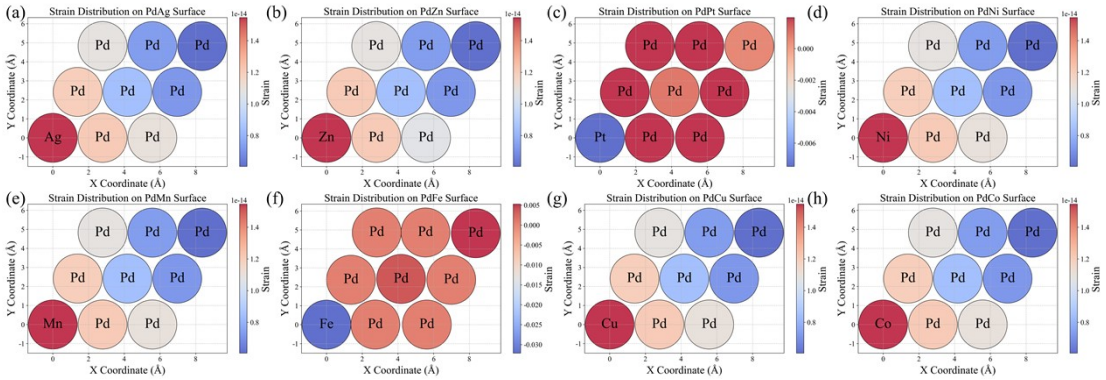

Figure S2. Atomic-scale strain distribution maps of Pd(111)-M Alloy Surfaces (M = Mn, Fe, Co, Ni, Cu, Zn, Ag, Pt) surfaces. (Note: The surface local strain is defined as the relative deviation of the average metal–metal bond length in the dopant atomic neighborhood from the ideal Pd–Pd bond length of the pristine Pd(111) surface, following the formula: $\varepsilon_{local} = \frac{\langle d_{M-Pd} \rangle - d_{Pd-Pd}^{ref}}{d_{Pd-Pd}^{ref}}$. where $\langle d_{M-Pd} \rangle$ is the average bond length between the dopant atom M and its first-nearest neighbor Pd atoms; d_{Pd-Pd}^{ref} is the reference Pd–Pd bond length of the ideal Pd(111) surface (derived from the optimized structure of the undoped Pd(111) surface); ε_{local} is a dimensionless quantity, with positive values representing tensile strain and negative values representing compressive strain)

Table S1. Charge Density Difference (CDD) Maps and Bader Charge Quantification for CO_2 Adsorption Configurations on Pd(111) and Pd(111)-M Alloy Surfaces (M = Mn, Ni, Cu, Zn, Ag, Pt). (Note: Δe denotes the electron transfer variation before and after adsorption, where positive values represent electron gain and negative values represent electron loss.)

	Pd(111)-Ag	Pd(111)-Cu	Pd(111)-Mn
CDD	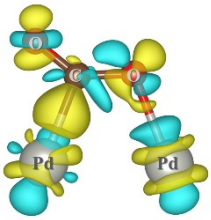	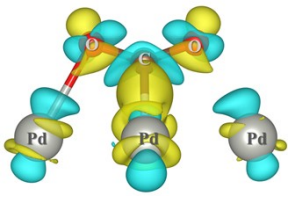	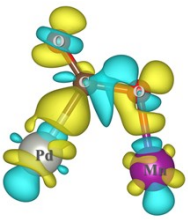
Δe(C)	0.78989	0.50328	0.813665
Δe(O1)	-0.132838	0.03124	-0.12353
Δe(O2)	-0.106362	0.04164	-0.05571
	Pd(111)-Ni	Pd(111)-Pt	Pd(111)-Zn

CDD	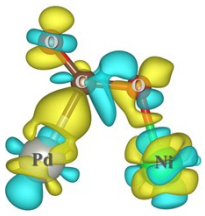	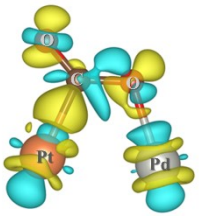	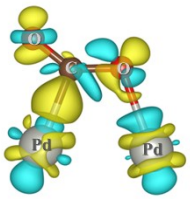
Δe(C)	0.749585	0.567096	0.749282
Δe(O1)	-0.10646	0.080489	-0.09632
Δe(O2)	-0.0781	0.010454	-0.11737
	Pd(111)		
CDD	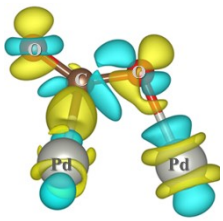		
Δe(C)	0.809908		
Δe(O1)	-0.08712		
Δe(O2)	-0.08509		

Table S2 C–O stretching vibration frequencies, structural parameters of Pd(111) and Pd(111)-M alloy surfaces (M = Mn, Fe, Co, Ni, Cu, Zn, Ag, Pt).

Catalyst	ν(C–O) (cm^{-1})	d(C–O) (Å)	∠(O–C–O) (°)
Pd(111)	1672.39	1.2764	135.58
Pd(111)-Ag	1788.86	1.2610	140.62
Pd(111)-Co	1746.26	1.2912	134.48
Pd(111)-Cu	1682.78	1.2460	138.48
Pd(111)-Mn	1729.59	1.3088	131.44
Pd(111)-Ni	1754.15	1.2822	135.22
Pd(111)-Pt	1707.22	1.2863	132.28
Pd(111)-Zn	1800.37	1.2572	139.68
Pd(111)-Fe	1768.86	1.2786	136.39

Table S3. Data Table of Energy Barriers (E_b, eV) and Reaction Energies (E_q, eV) for Elementary Steps in the CO_2 Hydrogenation Reaction Network on Pd(111) and Pd(111)-M Alloy Surfaces (M = Co, Fe, Mn, Ni, Cu, Zn, Ag, Pt).

Reaction	**Pd(111)**		**Pd(111)-Ag**		**Pd(111)-Co**	
	E_b	**E_q**	**E_b**	**E_q**	**E_b**	**E_q**
$CH_2O^*+H^*\rightarrow CH_2OH^*$	0.81	0.09	0.87	-0.03	1.13	0.72
$CH_2O^*+H^*\rightarrow CH_3O^*$	0.97	0.36	0.83	0.32	0.96	0.34
$CH_2OH^*+H^*\rightarrow CH_3OH^*$	0.92	0.28	0.71	0.12	0.70	-0.05
$CH_3O^*+H^*\rightarrow CH_3OH^*$	1.05	0.00	0.74	-0.23	0.93	0.32
$CHO^*+H^*\rightarrow CH_2O^*$	2.05	1.80	0.84	0.57	1.16	0.88

CHO*+H*→CHOH*	2.02	1.56	1.01	0.14	1.43	0.84
CHOH*+H*→CH_2OH*	0.89	0.33	0.97	0.40	0.83	0.76
CO_2*→CO*+O*	1.32	-0.47	1.87	0.05	0.77	-1.21
CO_2*+H*→COOH*	1.14	0.44	1.02	0.23	1.31	0.21
CO_2*+H*→HCOO*	1.47	0.52	2.21	0.67	1.12	0.32
CO*+H*→CHO*	1.74	0.63	1.60	1.60	1.72	1.10
CO*+H*→COH*	1.92	1.04	1.77	0.88	1.76	0.86
COH*+H*→CHOH*	1.50	1.14	1.13	0.86	1.33	1.08
COOH*→CO*+OH*	0.67	-0.68	0.78	-0.52	0.96	-0.94
COOH*+H*→HCOOH*	1.04	0.40	1.19	0.38	1.07	0.59
COOH*+H*→HOCOH*	1.06	0.84	0.74	0.24	1.02	0.43
H_2COOH*→CH_2O*+OH*	0.65	0.21	0.53	0.11	0.95	-0.39
H_2COO*+H*→H_2COOH*	0.68	-0.27	0.76	-0.24	0.77	-0.10
HCOOH*→CHO+OH*	1.09	-0.45	1.50	0.70	1.10	-0.43
HCOO*+H*→H_2COO*	1.99	1.74	1.65	1.35	1.63	1.42
HCOO*+H*→HCOOH*	0.80	0.33	0.59	-0.05	0.82	0.47
HCOOH*+H*→H_2COOH*	1.45	1.14	1.41	1.17	1.31	0.85
HOCOH*→COH*+OH*	0.74	-0.47	1.60	0.12	1.32	-0.50
OH*+H*→H_2O*	0.90	0.04	0.81	-0.12	0.40	0.28
O*+H*→OH*	1.38	0.23	0.60	-0.34	1.19	0.48
Reaction	**Pd(111)-Cu**		**Pd(111)-Mn**		**Pd(111)-Ni**	
	E_b	**E_q**	**E_b**	**E_q**	**E_b**	**E_q**
CH_2O*+H*→CH_2OH*	0.89	0.17	0.89	0.79	1.16	0.56
CH_2O*+H*→CH_3O*	1.07	0.35	0.86	0.28	1.09	0.36
CH_2OH*+H*→CH_3OH*	0.93	0.34	0.81	-0.13	0.63	0.07
CH_3O*+H*→CH_3OH*	1.09	0.17	0.84	0.38	1.00	0.28
CHO*+H*→CH_2O*	1.22	0.84	1.24	0.61	1.20	0.91
CHO*+H*→CHOH*	1.03	0.37	1.62	1.01	1.33	0.77
CHOH*+H*→CH_2OH*	1.11	0.65	0.39	0.38	0.82	0.70
CO_2*→CO*+O*	1.16	-0.43	0.19	-1.27	0.73	-1.00
CO_2*+H*→COOH*	1.14	0.34	1.27	0.59	0.91	0.07
CO_2*+H*→HCOO*	1.47	0.58	0.88	0.20	1.11	0.33
CO*+H*→CHO*	3.06	1.60	1.32	0.64	1.78	1.28
CO*+H*→COH*	1.94	1.47	1.69	0.76	1.73	1.00
COH*+H*→CHOH*	0.84	0.50	1.07	0.89	1.24	1.05
COOH*→CO*+OH*	0.57	-0.66	0.69	-1.26	1.41	-0.71
COOH*+H*→HCOOH*	1.35	0.65	0.50	-0.17	1.51	0.74
COOH*+H*→HOCOH*	0.45	0.42	0.78	0.24	1.18	0.66
H_2COOH*→CH_2O*+OH*	0.89	0.09	1.00	-0.64	0.97	-0.21
H_2COO*+H*→H_2COOH*	0.77	-0.16	0.63	-0.24	1.25	-0.10
HCOOH*→CHO+OH*	1.02	0.29	1.55	-0.44	0.82	-0.17
HCOO*+H*→H_2COO*	1.93	1.62	1.36	1.25	1.72	1.52
HCOO*+H*→HCOOH*	0.96	0.41	0.75	0.21	0.87	0.48

$HCOOH^*+H^*\rightarrow H_2COOH^*$	1.66	1.04	1.36	0.81	1.38	0.94
$HOCOH^*\rightarrow COH^*+OH^*$	1.40	0.38	1.47	-0.73	1.32	-0.38
$OH^*+H^*\rightarrow H_2O^*$	1.12	0.08	0.78	0.25	0.96	0.23
$O^*+H^*\rightarrow OH^*$	1.26	0.11	1.04	0.60	1.15	0.35
Reaction	**Pd(111)-Zn**		**Pd(111)-Pt**		**Pd(111)-Fe**	
	E_b	**E_q**	**E_b**	**E_q**	**E_b**	**E_q**
$CH_2O^*+H^*\rightarrow CH_2OH^*$	0.84	0.12	0.87	-0.01	0.79	0.19
$CH_2O^*+H^*\rightarrow CH_3O^*$	1.07	0.39	0.91	0.65	0.81	0.18
$CH_2OH^*+H^*\rightarrow CH_3OH^*$	0.93	0.29	1.03	0.62	1.18	-0.06
$CH_3O^*+H^*\rightarrow CH_3OH^*$	1.12	0.02	0.76	-0.04	0.71	-0.06
$CHO^*+H^*\rightarrow CH_2O^*$	1.19	0.78	1.19	0.89	1.23	0.64
$CHO^*+H^*\rightarrow CHOH^*$	1.10	0.33	0.84	0.36	1.68	0.55
$CHOH^*+H^*\rightarrow CH_2OH^*$	1.11	0.57	1.03	0.52	1.07	0.27
$CO_2^*\rightarrow CO^*+O^*$	1.25	-0.16	1.04	-0.48	2.05	-0.56
$CO_2^*+H^*\rightarrow COOH^*$	1.17	0.39	0.97	0.00	0.79	-0.08
$CO_2^*+H^*\rightarrow HCOO^*$	1.56	0.60	1.40	0.51	0.90	0.07
$CO^*+H^*\rightarrow CHO^*$	1.76	1.73	2.06	1.37	1.51	1.08
$CO^*+H^*\rightarrow COH^*$	1.97	1.12	1.85	0.89	3.51	1.37
$COH^*+H^*\rightarrow CHOH^*$	1.24	0.94	1.40	0.84	0.92	0.27
$COOH^*\rightarrow CO^*+OH^*$	0.60	-0.63	0.73	0.76	1.14	-0.52
$COOH^*+H^*\rightarrow HCOOH^*$	1.14	0.61	1.57	0.90	1.04	0.48
$COOH^*+H^*\rightarrow HOCOH^*$	0.93	0.42	0.89	0.25	2.75	0.61
$H_2COOH^*\rightarrow CH_2O^*+OH^*$	0.79	0.18	0.79	1.03	2.55	-0.09
$H_2COO^*+H^*\rightarrow H_2COOH^*$	0.80	-0.21	0.65	-0.32	1.07	-0.14
$HCOOH^*\rightarrow CHO+OH^*$	1.02	0.49	1.17	1.24	1.21	0.09
$HCOO^*+H^*\rightarrow H_2COO^*$	2.26	1.71	1.85	1.81	1.76	1.28
$HCOO^*+H^*\rightarrow HCOOH^*$	1.05	0.40	0.81	0.39	0.72	0.33
$HCOOH^*+H^*\rightarrow H_2COOH^*$	1.44	1.09	1.54	1.10	1.26	0.82
$HOCOH^*\rightarrow COH^*+OH^*$	1.34	0.07	2.70	1.41	2.36	0.24
$OH^*+H^*\rightarrow H_2O^*$	1.05	-0.01	0.20	-0.94	0.67	-0.13
$O^*+H^*\rightarrow OH^*$	1.12	-0.08	1.34	1.25	0.94	-0.04

Table S4. Adsorption Energies (eV) of Key Adsorbed Species on Pd(111) and Pd(111)-M Alloy Surfaces (M = Ag, Co, Cu, Mn, Ni, Zn, Pt, Fe)

	Pd(111)	Pd(111)-Ag	Pd(111)-Co	Pd(111)-Cu	Pd(111)-Mn	Pd(111)-Ni	Pd(111)-Zn	Pd(111)-Pt	Pd(111)-Fe
C*	-7.29	-7.31	-7.91	-7.22	-7.78	-7.58	-7.26	-7.45	-6.73
H*	-2.96	-2.83	-2.96	-2.99	-2.86	-2.99	-2.98	-2.96	-2.79
O*	-1.55	-1.07	-2.44	-1.51	-2.87	-2.09	-1.25	-1.57	-1.76
CO*	-2.19	-2.17	-2.32	-2.20	-2.17	-2.26	-2.21	-2.20	-2.11
H_2*	-0.76	-1.32	-1.39	-1.33	-1.18	-1.43	-1.34	-1.36	-0.01
CHO*	-2.84	-2.59	-3.38	-2.78	-3.53	-3.16	-2.65	-2.98	-3.01
CO_2*	-0.01	-0.03	-0.29	-0.03	-0.46	-0.09	-0.03	-0.02	-0.05
COH*	-1.84	-1.85	-2.16	-1.45	-1.95	-1.98	-1.80	-2.00	-1.26
CH_2O*	-0.55	-0.54	-1.14	-0.61	-1.47	-0.92	-0.53	-0.73	-0.84
CH_3O*	-2.35	-2.24	-2.96	-2.44	-3.24	-2.74	-2.32	-2.24	-2.65
CHOH*	-3.34	-3.27	-3.49	-3.39	-3.36	-3.37	-3.28	-3.56	-3.23
COOH*	-2.63	-2.73	-3.15	-2.78	-2.84	-2.97	-2.72	-3.09	-3.03
HCOO*	-2.67	-2.41	-3.14	-2.65	-3.33	-2.96	-2.62	-2.69	-2.98
CH_2OH*	-2.27	-2.23	-2.22	-2.26	-2.16	-2.18	-2.23	-2.54	-2.28
CH_3OH*	-0.26	-0.25	-0.55	-0.22	-0.69	-0.41	-0.23	-0.19	-0.45
H_2COO*	-4.06	-4.06	-4.87	-4.19	-5.11	-4.60	-4.07	-4.01	-4.67
HCOOH*	-0.38	-0.37	-0.72	-0.31	-1.06	-0.55	-0.28	-0.35	-0.53
HOCOH*	-2.64	-2.63	-3.00	-2.65	-2.77	-2.75	-2.59	-3.12	-2.52
H_2COOH*	-2.21	-2.05	-2.84	-2.26	-3.12	-2.61	-2.18	-2.22	-2.52
OH*	-2.75	-2.71	-3.39	-2.86	-3.60	-3.19	-2.77	-1.75	-3.06

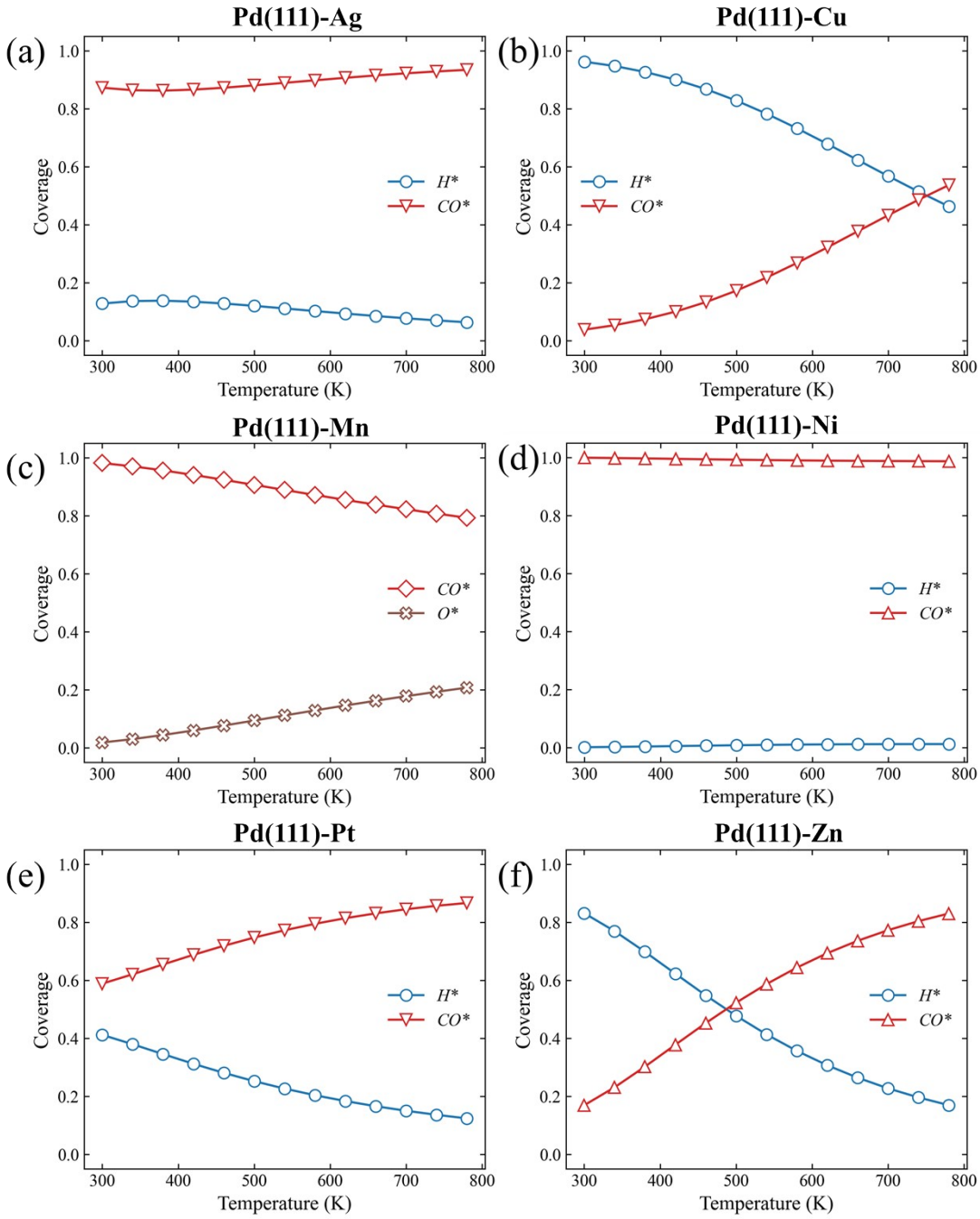

Figure S3. Surface Coverage of Main Adsorbed Intermediates (H*, CO*, O*) as a Function of Temperature (300–800 K) on Pd(111)-M Alloy Surfaces (M = Ag, Cu, Mn, Ni, Zn, Pt).

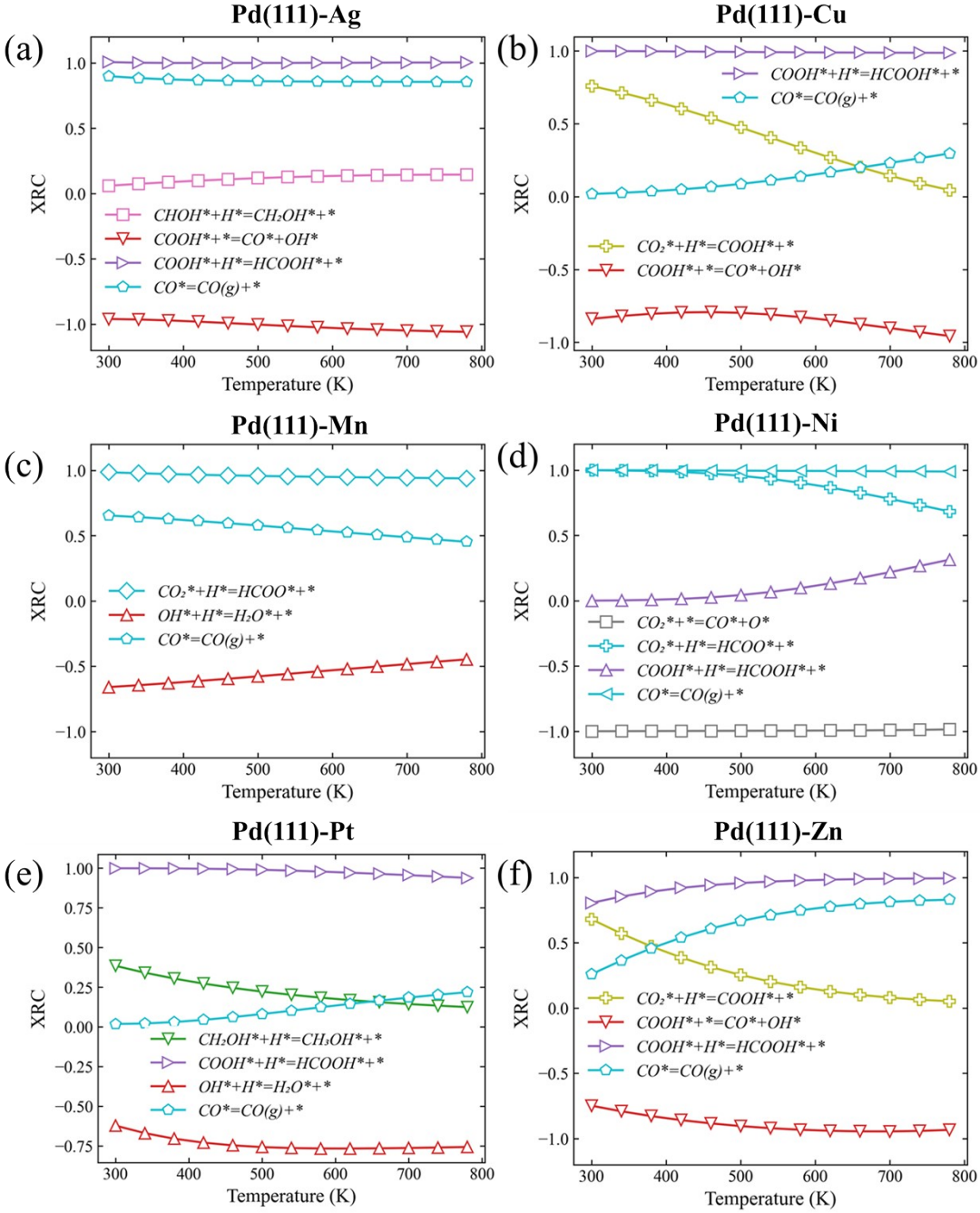

Figure S4. Degrees of Rate Control (XRC) for Elementary Steps in the CO_2 Hydrogenation Reaction as a Function of Temperature (300–800 K) on Pd(111)-M Alloy Surfaces (M = Ag, Cu, Mn, Ni, Zn, Pt)

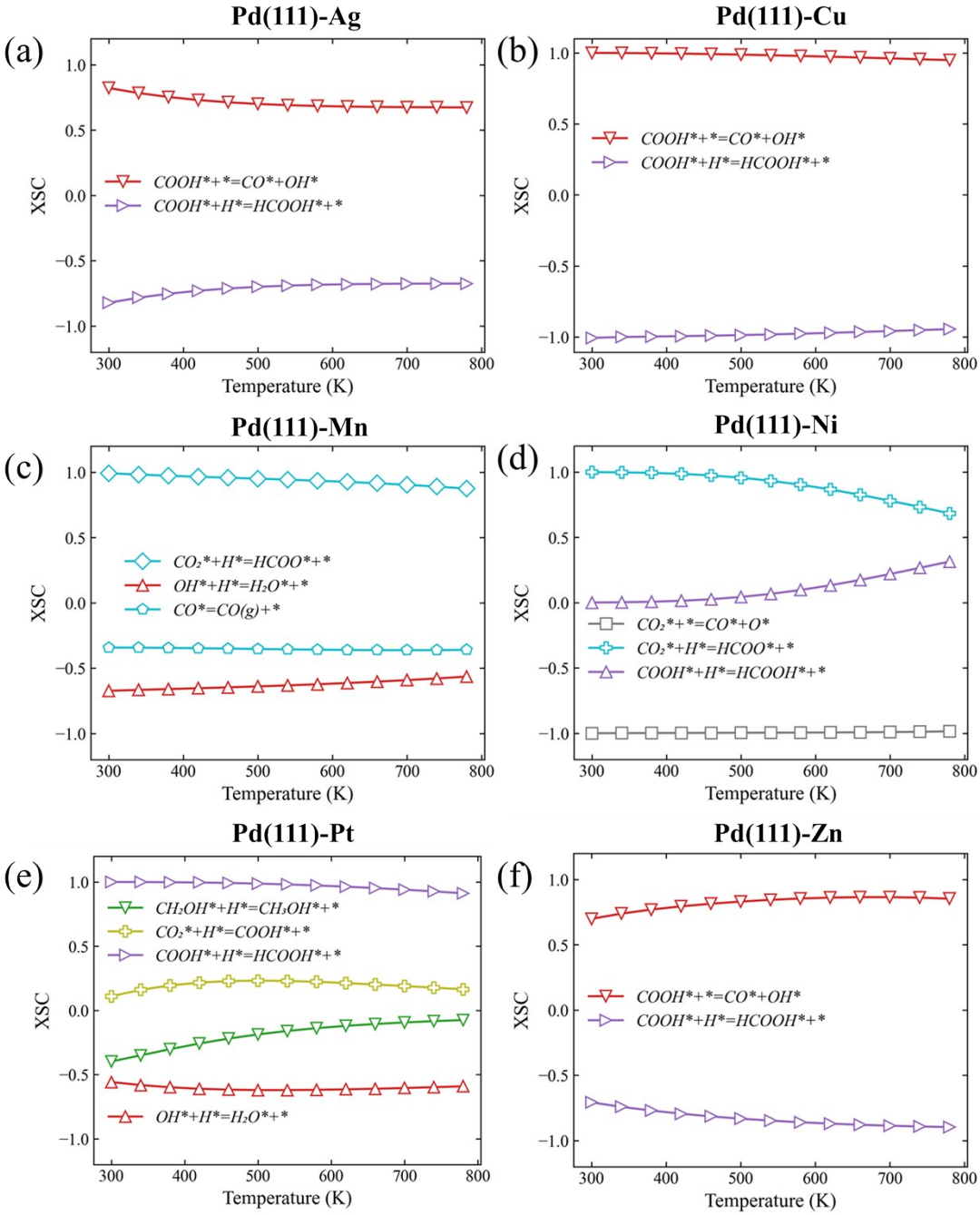

Figure S5. Degrees of Selectivity Control (XSC) for the Formic Acid (HCOOH) Product Pathway in the CO_2 Hydrogenation Reaction as a Function of Temperature (300–800 K) on Pd(111)-M Alloy Surfaces (M = Ag, Cu, Mn, Ni, Zn, Pt)

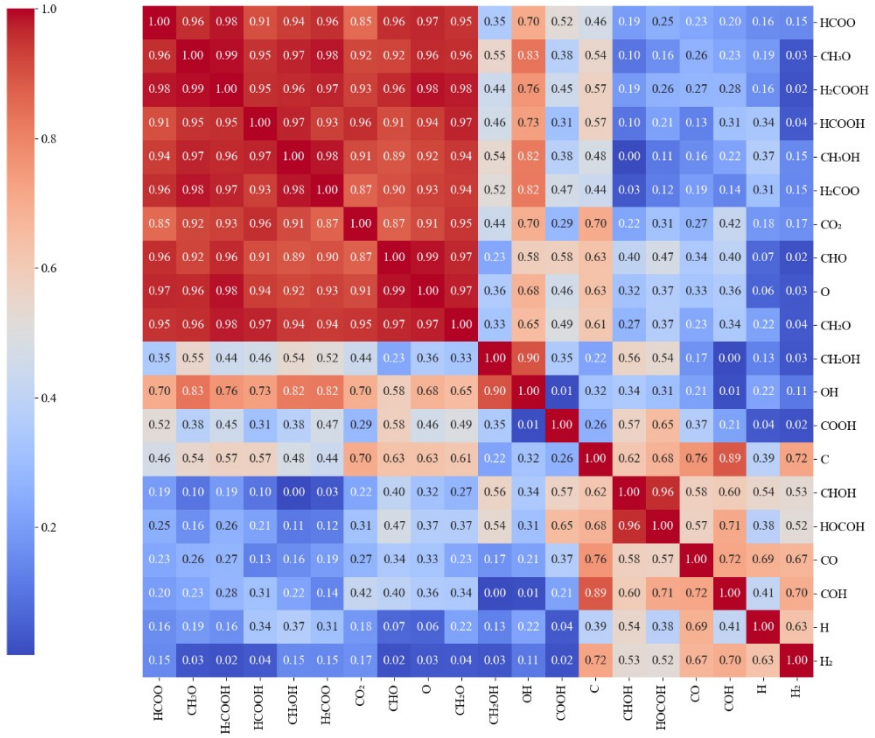

Figure S6. Bivariate Correlation Matrix Heatmap of Adsorption Energies for Adsorbed Intermediates in the CO_2 Hydrogenation Reaction on Pd(111) and Pd(111)-M Alloy Surfaces (M = Ag, Co, Cu, Mn, Ni, Zn, Pt, Fe)

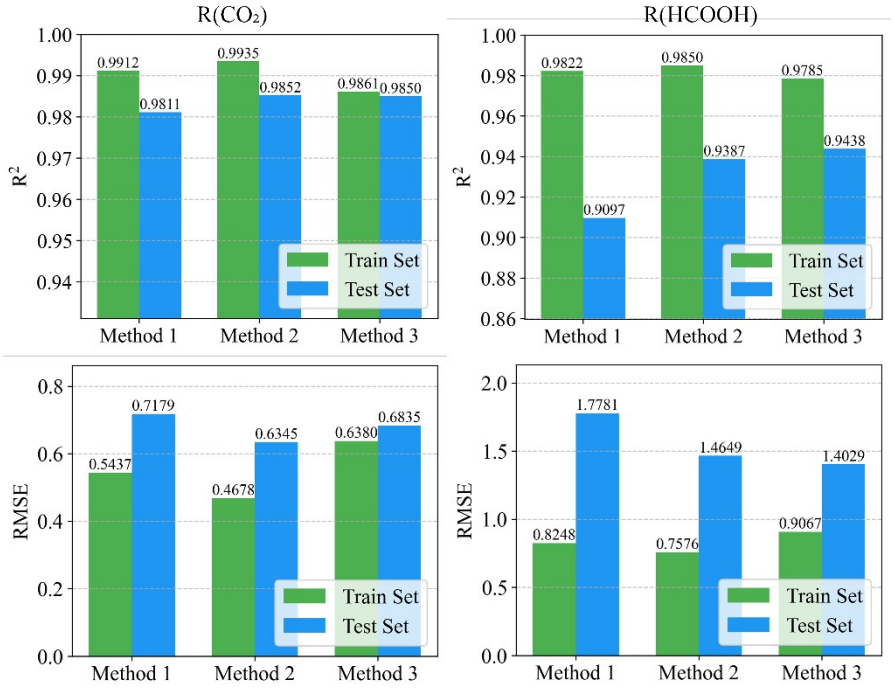

Figure S7. Performance Evaluation of SISSO Machine Learning Models with Three Preprocessing Schemes for Predicting CO_2 Consumption Rate (log R(CO_2)) and Formic Acid Formation Rate (log R(HCOOH)): R^2 and RMSE on Training and Test Sets

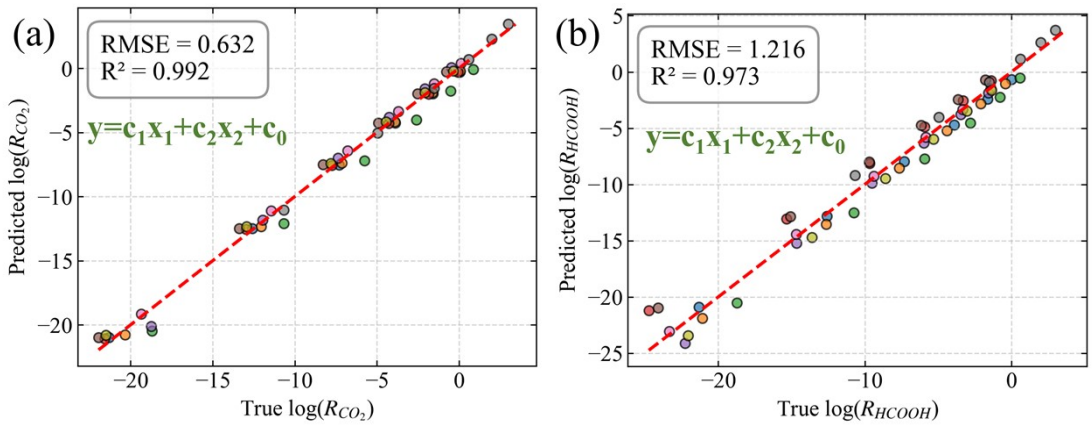

Figure S8. (a, b) Electronic structure descriptor-based parity plots for SISSO-predicted vs. microkinetic reaction rates of CO_2 consumption and HCOOH formation.

Table S5. The corresponding constants and descriptors in each expression, (Δq:Charge transfer amount of doped metals.ε_d:d-band center of doped metals.DOS_{ef}: Density of states at the Fermi level on the surface of Pd-based alloys.)

	log(R(CO_2))	log(R(HCOOH))
x_1	$\frac{1}{T\sqrt{\ln T}}$	$\frac{\exp(-\Delta q)}{T}$
x_2	$\frac{\Delta q \cdot DOS_{ef}}{T}$	$\left(\frac{\Delta q}{T\,\varepsilon_d}\right)$
c_0	12.115	11.4735
c_1	-114767	-9727.67
c_2	-3.7894	13644.67